Chapter 3

SiC(0001) cleaved surface reconstructions

3.1 Semiconductor surfaces

The formation of a surface in a material leads to interesting changes in the crystal and electronic structure near the surface. The basic reason is the loss of periodicity in one direction of the crystal lattice, which is responsible for the creation of electronic localized surface states, surface relaxation and reconstruction. These are very important properties; for example, they can be decisive in the adsorption process of other species onto clean surfaces. The study of clean surfaces has been very productive in the past 40 years, leading to the creation of new fields with many subbranches [11]. The importance of new technologies in everyday life has underscored the importance of the semiconductor branch of surface science. In fact, the continuous miniaturization of electronic devices such as integrated circuits, optoelectronic and non-volatile memory devices, has made semiconductors a most important material for industry. The semiconductor silicon carbide (SiC) has gained much popularity in the scientific community relatively lately, although it was known already in 1907 that crystals of silicon carbide emit light when an electrical current passes through them, and it was used as detector crystal in early radio receivers [13]. Problems related with the growth of high quality SiC crystals slowed down the integration of this semiconductor in technologically important processes, and their solution still remain the major task in current research.

Nevertheless, silicon carbide possesses very interesting and peculiar material properties which make it superior to silicon in a wide range of applications. The fundamental characteristic of a semiconductor, the bandgap, has a value of E_g ∼3 eV for SiC and is hence about three times larger than that of Si. This allows device operation up to many hundred degrees C, while the operation temperature of Si-based electronic devices is limited to 150°C. Operation at elevated temperatures simplifies power dissipation problems and reduces cost. The high value of its band gap allows the production of blue light emitting diodes (LED), although GaN or InGaN are now preferred, but SiC is still useful as a substrate. A high thermal conductivity guarantees homogeneous heat distribution in devices and also a fast heat transfer to the mounting of the device. One more peculiar property of SiC-based devices is the possibility to operate them at much higher voltages than silicon ones, making the handling of high voltage direct currents much easier in energy transmission and distribution networks [14]. The cheap delivery of electrical power is an important issue in modern society. The extensive utilization of power electronics with improved properties such as, for example, switching at high frequencies, low losses and low manufacturing costs will be of extreme importance in the future. Unfortunately, with the current available power semiconductor devices based on silicon, the possibilities to meet these requirements are limited. Therefore, SiC-technologies have become more and more important in the past decades and, since the problem of producing at low cost and in large quantity defect-free SiC wafers now appears to be resolved, they will probably substitute Si-based devices in many applications.

In a SiC crystal each atom is covalently bound to four atoms of the other chemical species in a tetrahedral coordination. The Si-C bonds are arranged in a hexagonal bilayer with carbon and silicon in alternating positions. The bilayers are stacked on top of each other along the direction perpendicular to the bilayer. The tetrahedral arrangement of Si-C bonds can be continued in two orientations differing by a 60° rotation. The different stacking sequence produces SiC crystals with various structural modifications called polytypes [15]. There are two extreme cases of the various possibilities, one is obtained when all the bilayers are oriented in the same direction and the corresponding crystal possesses a zinkblende structure; this corresponds to the cubic SiC modification and is called β-SiC. The other extreme case

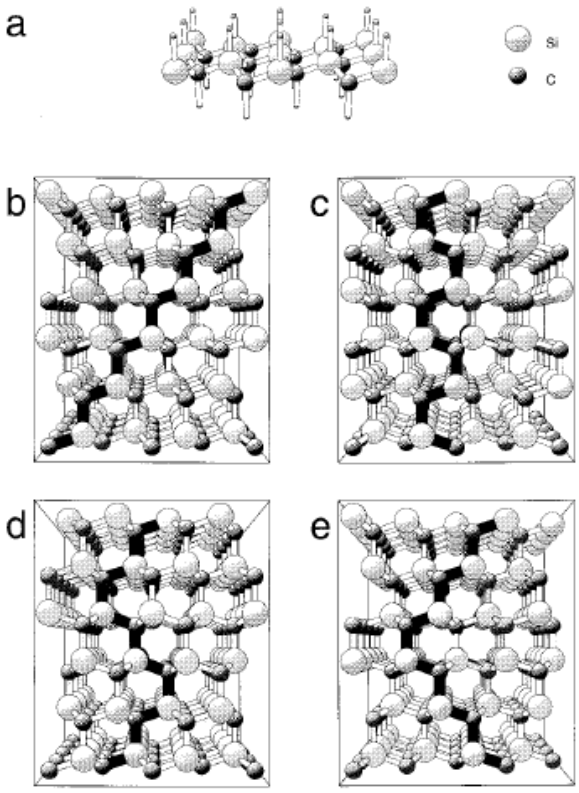

Figure 3.1: Four examples of Si-C bilayers stacking sequences. Changing the stacking sequence, different polytypes are formed. After ref. [15].

is when for every bilayer the stacking direction is rotated by 60° and the resulting crystal modification is the hexagonal wurtzite structure. Between these two extremes, there are about 170 different SiC polytypes. They have completely different spatially oriented three-dimensional bulk unit cells, but their energy of formation is almost independent of the particular polytype [15]. The way to distinguish between different polytypes is to refer to the periodicity along the stacking direction: the zinkblende structure can be described by a planar hexagonal unit cell with a periodicity of three bilayers along the c-axis forming an ABC sequence, and is therefore called 3C-SiC. The wurtzite structure has an AB sequence and is called 2H-SiC. Here C and H are used to denote the cubic or the hexagonal unit cell symmetry. Most of the electrical applications have been reported for the 3C, the 4H and the 6H polytypes, while the 2H-SiC has not been observed to be stable in nature. The 4H-SiC has two bilayers of identical orientation followed by

two bilayers with the opposite orientation, with an ABCB sequence, while 6H-SiC has an ABCACB sequence and up to the third bilayer has the same sequence as the 3C-polytype. The hexagonal unit cell in the 4H and 6H polytypes has a height of 4 and 6 bilayers, respectively (see Figure 3.1).

3.2 Semiconductor surface reconstructions

The theory used to understand the crystal and electronic properties of solids is based on Bloch's theorem which is applicable to the ideal case of an infinite perfect periodic lattice. The surface breaks this periodicity in one direction, producing new features which are not present in the bulk solid.

These modifications are particularly interesting in the case of semiconductors, where the existence of a bandgap in the volume is altered in the region next to the surface: new states can be possible within the gap, modifying the properties to the surface. While in the case of metals the electrons are highly delocalized all over the crystal, semiconductor elements and compounds are characterized by the strong directionality of their bonds. In fact, the surface in a semiconductor crystal is created by breaking the bonds between atoms on the surface, producing a strong increase in the surface free energy, and, therefore, in its reactivity.

The occurrence of broken bonds (dangling bonds) is responsible for surface reconstruction and relaxation, which are frequently found on semiconductor surfaces. A typical example of surface reconstruction is given by the Si(111) surface with its two well-known reconstructions: the (7×7), which is a very complex reconstruction, and is explained by the dimer-adatom-stacking fault (DAS) model proposed by Takayanagi *et al.* [16] on the basis of electron microscopy, and later confirmed by STM. A less complex but, nevertheless equally intriguing reconstruction is the Si(111)-(2×1) reconstruction which is a metastable reconstruction. In fact, when heated up to 600 K it undergoes an irreversible transition to the already cited Si(111)-(7×7) reconstruction. The (2×1) reconstruction has been subject of a long and intense scientific debate in the late 70's. It was clearly observed for the first time in the famous work of Lander [17], where the low energy electron diffraction (LEED) pattern of a cleaved Si(111) surface exhibited extra spots in the mid-positions between the normal, integral order spots expected from the bulk crystals. They also observed that "*transitions to different struc-*

tures occur at higher temperatures" that were called Si(111)-5 and Si(111)-7. This was in a sense the beginning of modern surface science.

The (111) is the plane where cleavage in silicon and germanium is possible. It happens between two double layers as shown in figure 3.2(a), and produces only one dangling bond per unit cell, while in the other two high symmetry directions (110) and (100), the surface produces two dangling bonds per unit cell. A first attempt to give a theoretical explanation of the half order spot in diffraction was given by Haneman [18] in 1961 on the basis of experimental data of Schlier and Farnsworth [19]. He explained the occurrence of a primitive rectangular mesh as a result of a displacement of the surface atoms in a configuration where "*every second atom, counting along alternate close-spaced rows, is raised with respect to its neighbors, so that the actual surface layer consists of atoms whose spacing is exactly twice that of atoms in bulk (111) planes*". The consequences of such displacement are very strong in the bonding properties of the surface atoms. While in the bulk every atom is bound to three atoms by tetrahedral sp^3 bonds, the atoms raised in the direction perpendicular to the surface will experience an alteration of the quantum state of the dangling bond [18]. In this way, the total energy of the surface should be minimized, but the reconstructed surface becomes ionic. For many years this model was used to explain the (2×1) reconstruction in both silicon and germanium, although some experimental results were in clear contrast with its predictions. The most important disagreement between theory and the experiments were related to the ionicity of the surface. This predicts a large charge transfer between the atoms of the surface displaced in opposite directions. The charge transfer has to take place from the lowered atoms towards the raised ones. Tight-binding calculations gave in fact a net charge of -0.76e_0 on the raised, +0.36e_0 on the lowered and +0.4e_0 on the second layer atoms [20]. In agreement with the basic physics of core level spectroscopy, the large charge transfer should cause appreciable core level shifts [12], but photoemission experiments conducted between the end of the 70's and the beginning of the 80's [21],[22] revealed little shift, a sign that the charge transfer was much lower than that predicted. The estimate of the charge transfer, responsible for the core level shifts, gave approximately 0.15e_0 which is much smaller than the 0.76e_0 calculated for the buckled reconstruction [21]. The solution to the puzzling (2×1) surface reconstruction of Si(111) and Ge(111) was later given

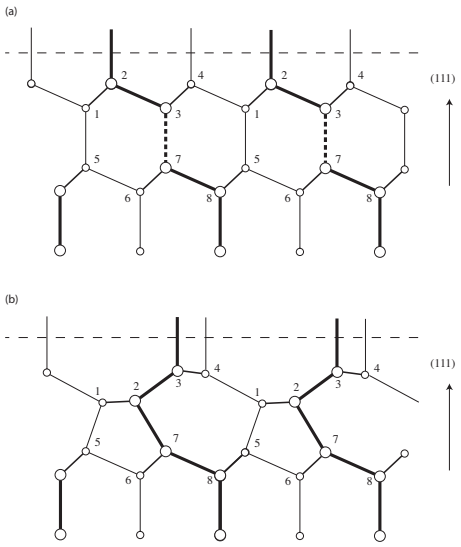

Figure 3.2: (a) ideal 1×1 termination after cleave along the line. (b) Pandey model of the 2×1 reconstruction. The bond between atoms #3 and #7 breaks and the bond #2-#7 is formed. In the 2×1 reconstruction the distance between the two pairs of dangling bonds is 2 times the distance in the ideal cleaved surface.

by Pandey [23], who proposed a new model based on π-bonded chains. A description of this model is given in Figure 3.2.
According to Pandey, the (2×1) LEED pattern does not result from a buckling of the surface but from a more general rearrangement of the atoms of the first two bilayers. This rearrangement happens through breaking of bonds (between the atoms #3 and #7 in figure 3.2) and creation of new ones (between the atoms #2 and #7). This new model predicts a non-polar surface reconstruction, in agreement with the core-level results and with other experimental results: with angle-resolved photoemission experiments that showed a large distance between surface atoms in one direction of the surface unit cell and a small one in perpendicular direction [24]; and with surface differential reflectance (SDR) experiments which gave as result a strong absorption with light polarized along the $(\bar{1}10)$ direction and no signal with a polarization along the $(\bar{2}11)$ direction [25].

3.2.1 The IV group elements and the IV-IV compound semiconductors

The similarity between silicon carbide and the IV group semiconductors results mainly in an identical nearest-neighbour configuration, which also in SiC is tetrahedral with a bond length of 1.89 Å. The major difference lies in

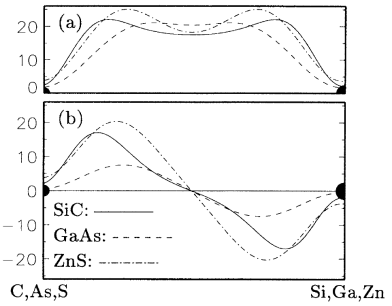

Figure 3.3: Symmetric (a) and antisymmetric (b) components of the total valence charge densities of GaAs, SiC and ZnS along the anion-cation bonds. After ref. [28].

the ionic nature of the Si-C bond, due to the extreme disparity of the covalent radii of Si (r_{Si}=1.17 Å) and C (r_C=0.77 Å) which originates from the different strength of the Si and C potentials. The ionic nature of the Si-C bond can be also understood in terms of the large difference of electronegativity of the two elements (e_{Si}=1.7; e_C=2.5), leading to a charge transfer from Si to C atoms [26]. The ionicity of SiC gives rise to an ionic gap within the valence bands of the bulk-band structure, similarly to the case of III-V and II-VI heteropolar compound semiconductors. In SiC, hence, the Si atoms act as cations and the C atoms as anions. It is interesting to compare the ionicity of SiC with that of the III-V heteropolar semiconductor GaAs and the II-VI ZnS. To do this, it is appropriate to use the Garcia-Cohen scale, which gives, through the g value, the ionicity of many compounds taking into account the asymmetry of the charge density along the bonds [27]. It has been demonstrated that SiC is in some sense more similar to the heteropolar ionic compound ZnO than to the heteropolar covalent semiconductors GaAs and ZnS [28]. Calculations of the symmetric and antisymmetric components of the charge densities of GaAs, SiC and ZnS along the anion-cation bonds, predicted that the maximum position of the antisymmetric component is shifted closer to the anion in SiC than in GaAs or ZnS, and is similar to the case of ZnO (see Fig. 3.3). This asymmetry in the charge density of the two elements Si and C is one of the reasons for the distinctively different reconstruction behaviour of the Si- and C-terminated surfaces [26]. Due to the charge asymmetry, the angular forces occurring at the Si and C atoms are largely different. They are much larger at the C than at Si atoms, so that changes of the tetrahedral configuration around the C atoms involve much more energy than for Si atoms. Another difference between diamond, silicon and silicon carbide is the lattice constant. For C,

the bulk lattice constant is a_C=3.57 Å, and for Si it is a_{Si}=5.43 Å, while for SiC it has an intermediate value a_{SiC}=4.36 Å. This is very important in the surface reconstruction; at Si- (C-)terminated surfaces one encounters Si (C) orbitals on a two-dimensional lattice with a lattice constant that is much smaller (larger) than that of related silicon (diamond) surfaces. This can produce a substantial difference in the reconstruction behaviour of SiC surfaces with respect to the Si and the C surfaces. It is, therefore, of great interest to investigate how decisive these differences between SiC and the IV group seminconductors are, with respect to surface reconstructions and electronic properties.

3.2.2 6H-SiC(0001) polar surface

The most studied SiC polytypes are the 3C- and the 6H- which are identical in the stacking direction up to the fourth bilayer. For surface sensitive experimental techniques, the 3C-SiC(111) and the 6H-SiC(0001) surfaces are, therefore, indistinguishable. Most reconstruction models for these polar surfaces involve Si and C adatoms or trimers and may therefore be called adsorption-induced reconstructions. The reconstruction is strongly dependent on the surface preparation procedure, which in the case of SiC can be more complicated than for many other materials, and is dependent on the surface termination. Ion bombardment, for example, has been used in various studies on the Si-terminated surfaces, providing an atomically clean surface with a stoichiometry near to a 1:1 ratio of silicon and carbon [29], and therefore usually denoted as a "stoichiometric surface". However, after ion bombardment, the surface presented a strong disorder, which could be removed only by annealing. This procedure produces a depletion of silicon because of the larger vapor pressure of silicon compared to carbon. A stoichiometric, well ordered surface is, therefore, not easily achieved by using a simple sputter/anneal preparation procedure.
Chemical methods and more complex thermal treatments are needed to obtain well ordered surfaces (see ref. [15] and references therein). A prolonged heating in oxygen at atmospheric pressures and temperatures around 1000°C, and subsequent covering of the surface with an oxide layer removable by HF etching, was shown to yield well ordered and stoichiometric surfaces. The limitation of this method consists in the necessity of removing the oxide

cap outside of the UHV chamber. A possible alternative to HF etching is to anneal the samples in UHV. The problem is again carbon enrichment as mentioned above, which can be partially reduced by lowering the anneal temperature to 850°C. Another alternative is to evaporate silicon on the sample during annealing at 1000°C in order to compensate for the Si loss during annealing. It is clear that in this case the resulting surface structure strongly depends on the balance between the silicon depletion caused by the temperature treatment and the silicon compensation. This led to the observation of many different surface reconstructions. On the 3C-(111) and nH-(0001) surfaces, the stable reconstruction is the (3×3), which is Si-rich, but upon lower silicon flux or higher temperature annealing a C-rich $(\sqrt{3}\times\sqrt{3})-R30°$ phase can be obtained [15]. Upon further annealing, a $(6\sqrt{3}\times 6\sqrt{3})R30°$ has been observed, composed of several coexisting phases of different order. The C-terminated $(000\overline{1})$ surface also has various reconstructions, such as the (1×1) after preparation under Ga flux at elevated temperatures and, upon further annealing, the $(\sqrt{3}\times\sqrt{3})$ phase. Also a carbon rich (3×3) reconstruction prepared by annealing has been found to be stable; upon further heating it transforms into a $(\sqrt{3}\times\sqrt{3})$ structure. The atomic structures of these various reconstructions are usually very complex and for many of them there is no complete agreement between the various investigations and the theoretical models yet, also because the particular atomic structure can be different for the various preparation procedures, even though the LEED images show the same symmetry. An example is the Si-rich (3×3) for which two models have been proposed (shown in Fig. 3.4) and for which the debate is still open [15]. The electronic structure of these reconstructions is equally puzzling and many experimental as well as theoretical investigations have been performed in the last years [30], but in many aspects no general agreement has been found. One particular question concerns the electrical character of the surface. All the above mentioned reconstructions have an odd number of electrons in the surface unit cell, which produces half-filled surface bands, conferring a metallic character to the surfaces. On the other hand, the experimental results show that the surfaces are semiconducting, in clear contrast to the simple electron counting rule. To resolve such discrepancy, it has been necessary to introduce electronic correlation, with a lower and upper Hubbard band, which gives to the $(\sqrt{3}\times\sqrt{3})$, for example, a semiconductor character.

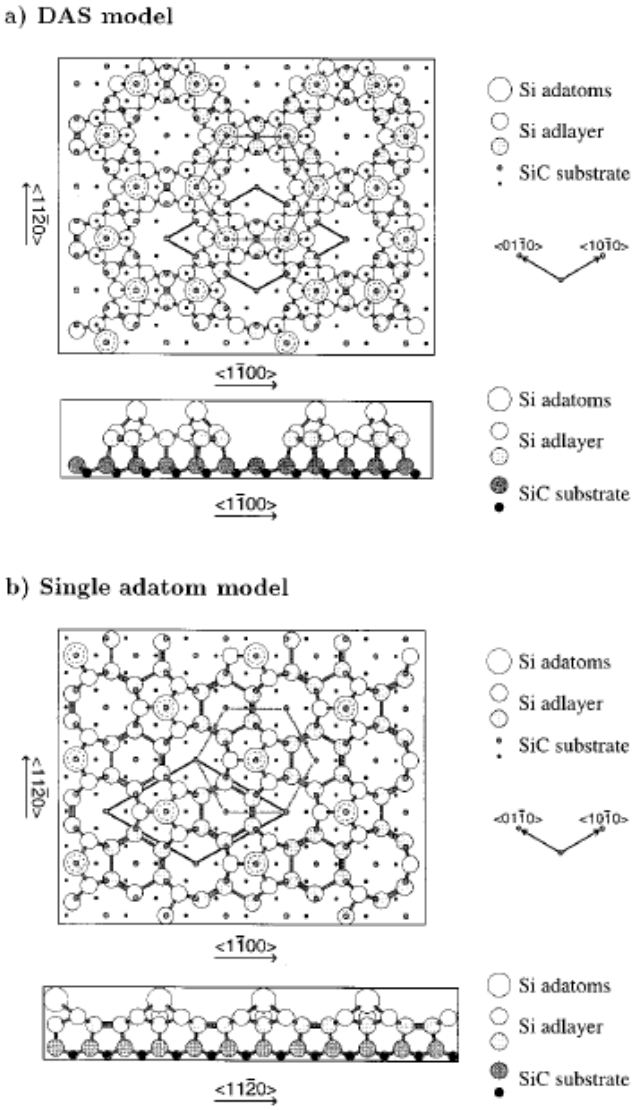

Figure 3.4: Example of two (3×3)-6H-SiC(0001) reconstruction structural models. The dimer-adatom-stacking fault (DAS) model was proposed by Kaplan (a) and the single adatom model by Kulakov *et al.* (b). After ref. [15].

The difficulty to find a standard procedure in preparing the clean surfaces of SiC, and the use of techniques which cannot be well controlled, such as

annealing under silicon flux, has caused a great amount of experimental work which led to different and sometimes contrasting results, making the study of the various reconstructions of the SiC surfaces very difficult. A way to overcome these problems is to produce the clean surface in a more *direct* way, without using any annealing, sputtering or etching procedures. This can be thought of as a going back to the origin of modern surface science, taking advantage of the simple technique of cutting ("cleaving") the sample in UHV. The (0001) planes can be cleaved, in fact, producing one dangling bond per unit cell, when the cut is performed between two bilayers, similar to the case of Si, Ge and C(111) surfaces. The creation of the surface by cleaving is more difficult in SiC than in Si, because the Si-C bond is stronger than the Si-Si bond, but it is still possible. Indeed, here we report on the first study of cleaved SiC surfaces.

3.3 Experimental set up

Photoemission experiments have been carried out at the UE-56/2 beamline at the BESSY storage ring, in a typical UHV chamber with a base pressure of 1×10^{-10} mbar. Photoelectrons were analyzed in an angle-resolving hemispherical analyzer, Omicron AR65, equipped with three channeltron detectors. The total experimental resolution was set to 100 meV for the Si $2p$ core level and to 200 meV for the C $1s$. All spectra were taken with an angle of incidence of 30° and at normal emission with an angular acceptance of about 1°.

The chamber was equipped with a LEED optics by means of which the surface symmetry was determined. The primary electron energy could be varied remotely from a computer in a wide range (50-300 eV) and the image was recorded by a CCD camera, in order to obtain I(E) profiles of symmetry points.

The samples were bulk 6H-SiC heavily-doped with nitrogen (n-type) as revealed by their dark colour. In order to avoid charging during photoemission experiments, an ohmic contact was formed with indium, with a resulting resistance as low as 500 Ω.

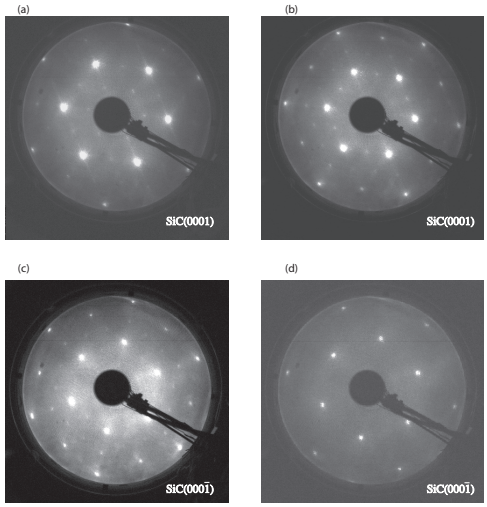

Figure 3.5: LEED patterns of the Si and C-terminated surfaces: the primary electron energies are 113 eV (a), 162 eV (b), 170 eV (c) and 135 eV (d).

3.4 6H-SiC(0001)(2×1): experimental results

3.4.1 LEED

Samples of 6H-SiC were cleaved in UHV along the (0001) direction and *in-situ* studied by means of LEED. Four LEED pictures corresponding to the two terminations of the SiC surface are shown in Fig. 3.5. In the following, the Si-terminated surface will be indicated as (0001), while the C-terminated one as (000$\bar{1}$). The presence of extra spots in the half-integer order positions of the LEED pattern is evident in Fig. 3.5, although their intensities are lower than those of the integer order ones. These (2×2) LEED patterns may represent either a true (2×2) superlattice or a superposition of three rotational domains of a (2×1) phase. The difference between the two possibilities lies in the equivalence of the spots of the $\left(\frac{1}{2}\frac{1}{2}\right)$ order in the first case, while in the case of three domains the half order diffraction spots are inequivalent, because spots from the same domain are in the opposite position with respect to the $\left(00\right)$ spot and in principle the occurrence of the different domains is inequivalent. Therefore, the spot intensity has been inspected in the following way: half-order spots at opposite positions are shown in the boxes in Fig. 3.6(left) with the same colour frames. Their intensities are plotted as a function of the primary electronic energy on the right in the same figure. The profiles look very similar in the sense that

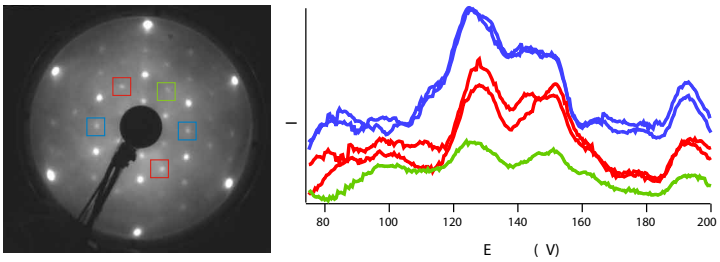

Figure 3.6: (left) LEED image taken on the C-terminated surface with 147 eV. (right) I(E) spectra (intensity vs energy curves) from individual half-integer spots plotted on identical scale. The colors of the curves are referred to the colors of the boxes of the LEED image (left).

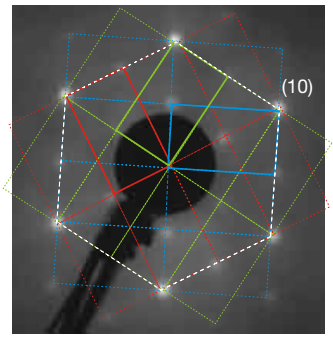

Figure 3.7: Same LEED image of Fig. 3.6. Three domains 2×1 reconstruction is responsible for the 2×2 LEED pattern observed on both termination surfaces. Here it is shown how the three domains are arranged to form the 2×2 pattern.

the peaks are located at similar energy positions, but the intensity of the peaks depends on the particular spot taken. In addition, the intensities are similar for every pair. This is the conclusive evidence that the spots are inequivalent but are coupled in a way corresponding to a three-domain (2×1) reconstruction. It is also clear from the difference in the spot intensities that the population of the three domains is different and that they are rotated by 60° (see Fig. 3.7). This result suggests a strong similarity with the case of the Si(111), Ge(111) and C(111) metastable (2×1) reconstructions. This is already a very important and unexpected result. It is the first time that a reconstruction involving an even number of atoms in the unit cell has been observed for SiC. It is therefore interesting to study in further detail the way this (2×1) reconstruction occurs. In the next section results from core level spectroscopy are shown, providing more information on the crystal and electronic structure.

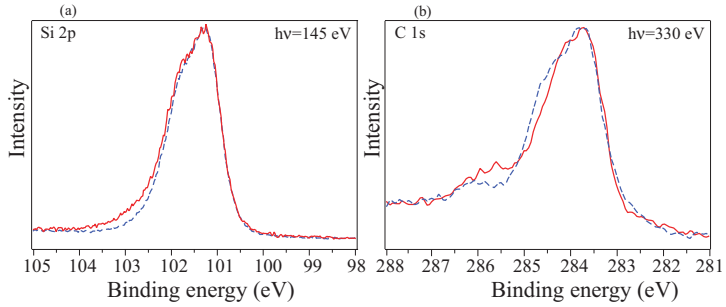

Figure 3.8: Si-2p (a) and C-1s (b) core level PE spectra of the C-terminated surface. Dashed lines correspond to spectra taken just after a new cleave; continuous lines to spectra taken after 80 minutes.

3.4.2 Core level spectroscopy

Our core level spectroscopy experiments have been performed after *in situ* cleaving the SiC sample. The samples, cleaved at a pressure of 4×10^{-10} mbar, were quickly transferred to the measurement position. The complete alignment of the samples with the photon beam and the analyzer was performed within 15 minutes after the cleave. The clean surface presented chemical reactivity as is clear from Fig. 3.8, where the Si 2p (Fig. 3.8(a)) and the C 1s (Fig. 3.8(b)) core level spectra of the SiC$(000\bar{1})$ surface are shown. The dashed lines are referred to the just cleaved surface and the continuous ones after 80 minutes. The appearance of an extra shoulder on the higher binding energy side in the spectra taken after 80 minutes is due to contamination as is clear from the width and the energy position. In fact, contamination with either hydrocarbons or oxygen results in peaks at higher binding energies with respect to the bulk core level of both Si 2p and C 1s. In Fig. 3.9 we show the peaks of the two species for the (0001) and the $(000\bar{1})$ surfaces. The first evidence is that, while the Si 2p core levels are very similar for the two surfaces, the C 1s spectra show strong differences: a new peak around 284.5 eV and a broad feature at 286 eV. The main C 1s peak has a binding energy of 283.6 eV, i.e. more than 1 eV shifted towards lower binding energy with respect to the C 1s bulk peak of diamond [31]. The Si $2p_{3/2}$ component of the Si 2p doublet has a binding energy of 101.2 eV, showing a shift of 1.4 eV towards higher binding energy. These shifts are due to the difference in electronegativity between Si and C, leading to

a charge transfer from silicon to carbon atoms, i.e. silicon atoms behave as cations and carbon atoms as anions. The values we have found are in good agreement with previous photoemission experiments on 6H-SiC(0001) and 3C-SiC(111) surfaces [32] and will be considered from now on as reference for the surface core level shifts. In Figs. 3.10 - 3.13 the line shape analysis by means of a least squares fitting procedure are shown. Lorentzian peaks numerically convoluted by a Gaussian (for the description of instrumental and phonon broadening) are used to model the photoemission lines. Typical Lorentzian widths of the C 1s and Si 2p are, respectively, 0.3 eV and 0.15 eV, as known from previous photoemission studies on SiC [33]. These are used to determine the Voigt line shape, taking Gaussian values as large as 0.8 eV for the C 1s and 0.65 eV for Si 2p. These large values for the Gaussian widths are probably due to the disorder on the surface, which is produced by the cleaving, with a large density of steps. The spin-orbit splitting for the Si 2p doublet is fixed to 0.608 eV with a statistical ratio of 0.5 and the symmetry factor for all the spectra is zero. The results of the fitting procedure are reported in table 3.1.

SiC(0001): The Si 2p spectrum of the Si terminated surface has three components; the bulk (B), the S_1 at higher binding energy and the S_2 at lower binding energy. The latter could be due to the dangling bond of the Si atoms at the surface (see Fig. 3.10). The C 1s core level shows three main components: the bulk (B) and the surface related S_1 and S_3 components (see Fig. 3.11). Here the S_1 component has a slightly stronger intensity compared to the S_3 one. The weak component (S_2) at higher binding energy

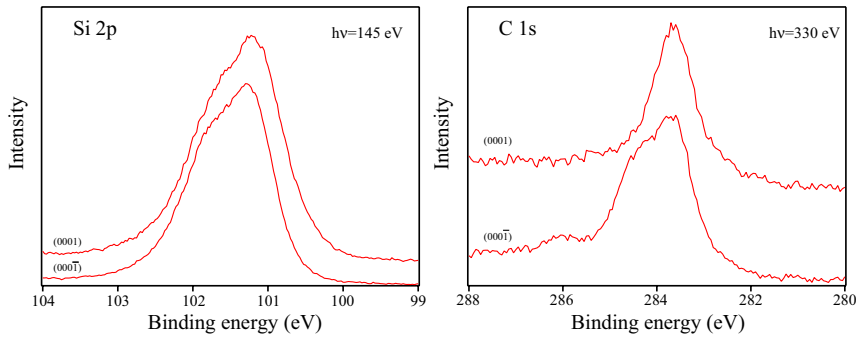

Figure 3.9: Si-2p (left) and C-1s (right) core level spectra recorded, respectively, at 145 eV and 330 eV for the C-terminated and the Si-terminated surfaces.

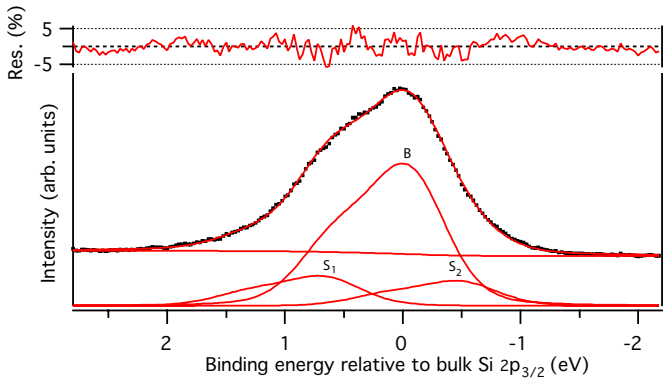

Figure 3.10: Silicon face: Si2p. Bulk Si2p=101.2 eV; S_1=101.9 eV (+0.7 eV); S_2=100.7 eV (-0.5 eV). Lorentzian width for all peaks= 0.15 eV. Gaussian for all peaks = 0.65 eV.

is probably due to sample contamination: it is always present, even in the just cleaved surfaces.

SiC(000$\bar{1}$): The C 1s spectrum on this surface termination is more complex compared to the one obtained from the other termination: it is characterized by the presence of one strong peak at higher binding energy, a peak with a very large shift (-2.4 eV) and a weak component at lower binding energy. The particularity of the C 1s for this termination is the strong intensity of the component at 0.9 eV which has no analogy in any of the other core level spectra, hence making clear the difference of the two reconstructions. The Si 2p spectrum of this termination has a component at higher binding energy similar to that of the Si terminated surface, but no component at lower binding energies (Fig. 3.13).

3.4.3 Discussion

The intensity and core level shift is related to the position and the bond geometry of the Si atom: reconstruction models have to be in agreement with these experimental properties. The starting point of our discussion could be the Pandey model which described successfully the (2×1) reconstructions of C, Si and Ge (111) surfaces. This model predicts a displacement of the atoms from the first two layers: in Fig. 3.14 the atomic structures of the bulk truncated and of the possible Pandey reconstruction for both surface terminations are depicted. Clear is the symmetric behaviour of the

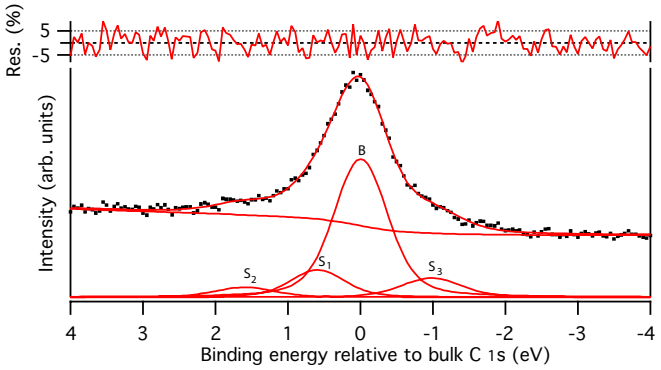

Figure 3.11: Silicon face: C1s. Bulk C1s=283.6 eV; S_1=284.2 eV (+0.6 eV); S_2=285.2 eV (+1.6 eV); S_3=282.6 eV (-1 eV). Lorentzian width for all peaks = 0.3 eV. Gaussian width = 0.7 eV; 0.7 eV; 0.8 eV; 0.8 eV.

Pandey reconstruction by exchanging the surface termination: the first two layers of each reconstruction are composed by both Si and C atoms; the only difference between the two reconstructions is a specular exchanging of the chemical species in the surface structure (see Fig. 3.14, (b) and (d)). Let us now try to relate this specular behaviour of the Si and C atoms with the core level spectra of both surface terminations. The two terminations are, at least in the first two layers, very similar; Si and C atoms in the first layer have a dangling bond and the other three bonds are with atoms of the

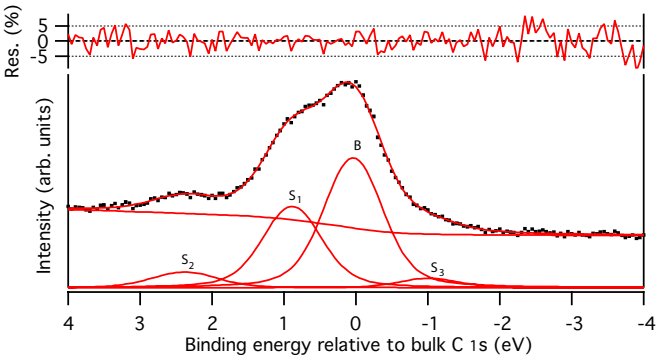

Figure 3.12: Carbon face: C1s. Bulk C1s=283.6 eV; S_1=284.5 eV (+0.9 eV); S_2=286.0 eV (+2.4 eV); S_3=282.6 eV (-1 eV). Lorentzian width for all peaks = 0.3 eV. Gaussian width = 0.8 eV; 0.8 eV; 0.9 eV; 0.8 eV.

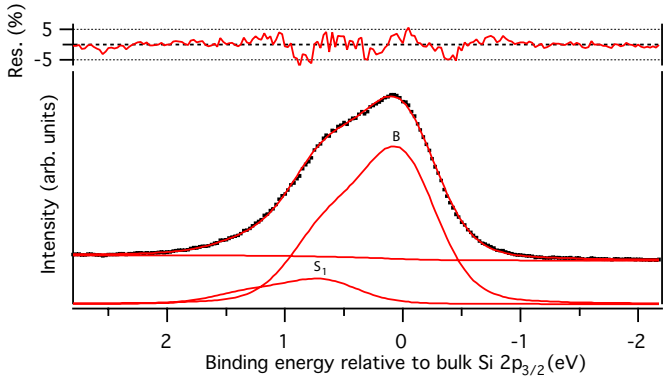

Figure 3.13: Carbon face: Si2p. Bulk Si2p=101.2 eV; S_1=101.9 eV (+0.7 eV). Lorentzian width for all peaks = 0.15 eV. Gaussian for all peaks = 0.65 eV.

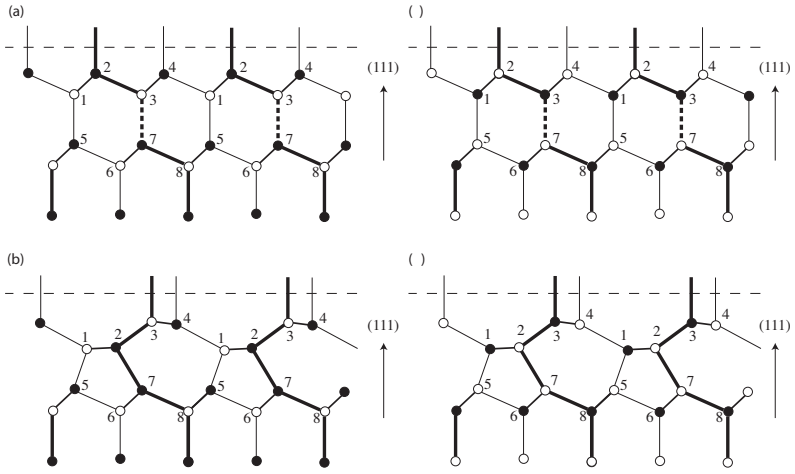

Figure 3.14: Stick and ball representation of the bulk truncated and of the possible Pandey reconstruction of 6H-SiC(0001) surfaces: a) and b) Si terminated; c) and d) C terminated.

other chemical species in the second layer. Hence the electronic properties of the atoms in the first two layers are very similar for the two terminations. Anyway, from the experimental core level spectra this similarity is not clear, at least the C 1s spectra are very different (see Fig. 3.9), with a strong surface component in the C termination. Moreover, both Si 2p and C 1s core level spectra should have surface components due to the dangling bonds in both surface terminations. For Si 2p the dangling bond causes a core level shift towards lower binding energies, while for C 1s the shift should be towards higher binding energies [1]. The symmetric geometry of the two reconstructions by exchanging the surface termination is broken by the nature of the bond between atoms from the second and the third layer. As can be observed in Fig. 3.14 (b) and (d), every second bond there is a homopolar (bond 2-7) Si-Si bond in the Si termination and C-C bond in the C-termination. These differences in the reconstruction geometry could explain the differences in the core level spectra. From an energetic point of view, it is possible, anyway, to predict that the C-C bond is more stable than a C-Si one. This means that, provided the energy necessary to break the C-Si bond is available, the resulting reconstruction is stable if a C-C bond is created. For the Si-termination, this is not true, in fact, the Si-Si bond is energetically less stable than the Si-C one. It seems that the two reconstuctions, although giving the same LEED pattern, are generated by two distinct processes.

3.5 Conclusions

In order to establish a possible similarity between SiC and other group IV elemental semiconductors, clean surfaces were obtained by cleaving. As shown by the LEED result, cleaved 6H-SiC{0001} surfaces are reconstructed in (2×1) periodicity. In particular, the LEED pattern has been related to the existence of three rotationally equivalent domains with different statistical populations.

[1] The creation of the surface breaks the bond between Si and C, leaving a dangling bond on the Si termination atoms. The charge equilibrium between the central silicon atom in the tetrahedral C_3Si-C basis and the carbon atoms is broken, now the silicon atoms on the surface recover back the charge that is coming from the dangling bond. This results in a core level shift towards lower binding energies.

Core level spectroscopy revealed a substantial difference of the (2×1) reconstructions compared with other reconstructions previously studied, and in particular it can be excluded in the (2×1) case, the formation of neither dimers nor trimers. One important aspect of the (2×1) reconstructions is their different nature on the two surface terminations as evidenced by the core level analysis. Anyway, a precise calculation of charge transfer and angular forces is needed in order to establish the real geometry of the reconstructions.